Energy Conversion and Management 149 (2017) 87–100

Contents lists available at ScienceDirect

Energy Conversion and Management

journal homepage: www.elsevier.com/locate/enconman

Review

A review on computational fluid dynamic simulation techniques for Darrieus vertical axis wind turbines

Masoud Ghasemian [a,*], Z. Najafian Ashrafi [b], Ahmad Sedaghat [c]

[a] Department of Mechanical Engineering, Bourns College of Engineering, University of California, Riverside, CA 92521, USA
[b] School of Mechanical Engineering, University of Tehran, Tehran 14395-515, Iran
[c] Department of Mechanical Engineering, Isfahan University of Technology, Isfahan 8415683111, Iran

ARTICLE INFO

Article history:
Received 15 May 2017
Received in revised form 27 June 2017
Accepted 6 July 2017
Available online 15 July 2017

Keywords:
Vertical axis wind turbine
Computational fluid dynamic
Darrieus
Power augmentation
Wind farm
Blade modification

ABSTRACT

The global warming threats, the presence of policies on support of renewable energies, and the desire for clean smart cities are the major drives for most recent researches on developing small wind turbines in urban environments. VAWTs (vertical axis wind turbines) are most appealing for energy harvesting in the urban environment. This is attributed due to structural simplicity, wind direction independency, no yaw mechanism required, withstand high turbulence winds, cost effectiveness, easier maintenance, and lower noise emission of VAWTs. This paper reviews recent published works on CFD (computational fluid dynamic) simulations of Darrieus VAWTs. Recommendations and guidelines are presented for turbulence modeling, spatial and temporal discretization, numerical schemes and algorithms, and computational domain size. The operating and geometrical parameters such as tip speed ratio, wind speed, solidity, blade number and blade shapes are fully investigated. The purpose is to address different progresses in simulations areas such as blade profile modification and optimization, wind turbine performance augmentation using guide vanes, wind turbine wake interaction in wind farms, wind turbine aerodynamic noise reduction, dynamic stall control, self-starting characteristics, and effects of unsteady and skewed wind conditions.

Published by Elsevier Ltd.

Contents

* Corresponding author.
E-mail address: mghas002@ucr.edu (M. Ghasemian).

http://dx.doi.org/10.1016/j.enconman.2017.07.016
0196-8904/Published by Elsevier Ltd.

1. Introduction

In the last decade, utilization of renewable energy sources have been accelerated due to global warming threats, depletion of fossil fuel sources, and stricter environmental regulations in global energy market and society [1]. Among all renewable energies, wind energy is considered to be the most cost-effective source and it has experienced a rapid growth globally [2]. The global cumulative installed capacity of wind power rose from 24 GW in 2001 to 487 GW in 2016 and is expected to reach 817 GW by 2021 (see Fig. 1). In 2016, as shown in Fig. 2, the new installed capacity of the worldwide wind power constituted the total of 54.6 GW with three major contributors as China (42.8%), U.S. (15%) and Germany (10%) [3].

Wind turbines can be classified into horizontal axis wind turbines (HAWTs) and vertical axis wind turbines (VAWTs) based on the rotation axis [4]. Although HAWTs continue to be the commercially viable for large-scale power production, VAWTs operate under low wind speed conditions which are favorable for micro-generation. VAWTs have recently received growing interest for energy harvesting in the urban environment [5,6]. This growing interest is due to lower manufacturing costs, simple blade profile and shape, lower installation and maintenance costs, having the generator installed at the ground level, lower noise pollution, and lower operational tip speed ratio. Moreover, VAWTs are more appropriate for high turbulent regions where unsteady and skewed wind conditions are prevalent. Another advantageous for VAWTs, there is no need to a yawing mechanism to adjust the rotor direction to the changing wind direction.

Generally VAWTs can be categorized into two types: Savonius and Darrieus wind turbines [7]. The Savonius rotor is a vertical axis wind turbine that operates under a differential drag between its buckets. The Savonius rotor is promising solution for low wind speed conditions, but it's efficiency is low [8]. On the other hand, Darrieus type wind turbines are lift type machines which have higher power performance compared to the Savonius rotors. To acquire a better insight into different wind turbines concepts, the power performance and operating range for different types of wind turbines are shown in Fig. 3.

Increasing studies are made towards improving the efficiency and to extend the applicability of wind turbines to all suitable locations [11]. The wind turbine performance and flow characteristics were studied experimentally and numerically. A number of numerical simulation techniques were developed from which the Vortex model, Blade Element Momentum (BEM), Multiple Streamtube Model, and Computational Fluid Dynamics (CFD) are highly cited. Analytical models such as Vortex model [12] and Multiple Streamtube Model [13] are based on one dimensional simplified equations which requires some measured data on the employed airfoil sections in terms of lift and drag coefficients. In addition, these simplified models do not consider information on the wakes and merely employ semi empirical equations to consider the tip vortex and dynamic stall effects. Since these models use the statistically determined airfoil data will fail to determine accurately when the airfoil experiences dynamic stall [14]. On the other hand, Computational Fluid Dynamic (CFD) technique has become a routine practice to research in wind energy and helped to design more efficient and productive wind turbines. CFD can be employed as a powerful tool to analyze, design, and optimize wind turbine blades. CFD can provide more accurate data of flow characteristics around wind turbines compared to the other numerical models.

Many review papers highlighted different aspects of wind turbines such as aerodynamics model for Darrieus wind turbine [15], fluid dynamics aspect of Savonius wind turbine [16], VAWTs airfoil design [17], small scale wind turbines [18], Darrieus VAWTs [19], performance enhancements on vertical axis wind turbines using flow augmentation systems [20], wind turbine noise mechanisms [21], wind turbine wake aerodynamics [22], computer aided numerical simulation techniques in wind energy [23]. But, the lack of a detailed review paper that addresses the computational fluid dynamic simulations in Darrieus VAWTs field is felt.

The current paper provides an extensive literature review on the Computational Fluid Dynamic simulation of Darrieus VAWTs.

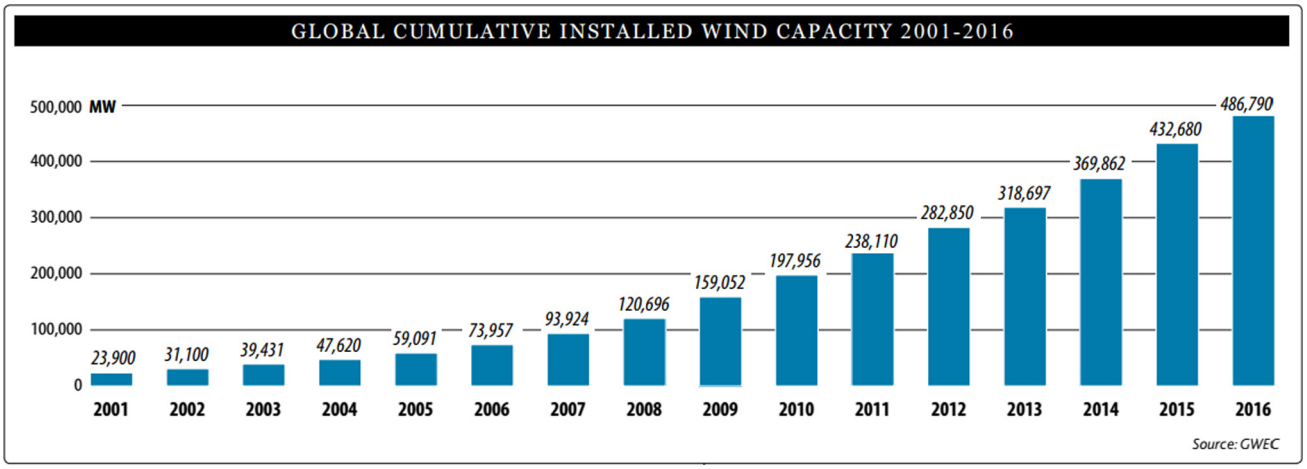

Fig. 1. Global cumulative installed wind capacity 2001–2016 [3].

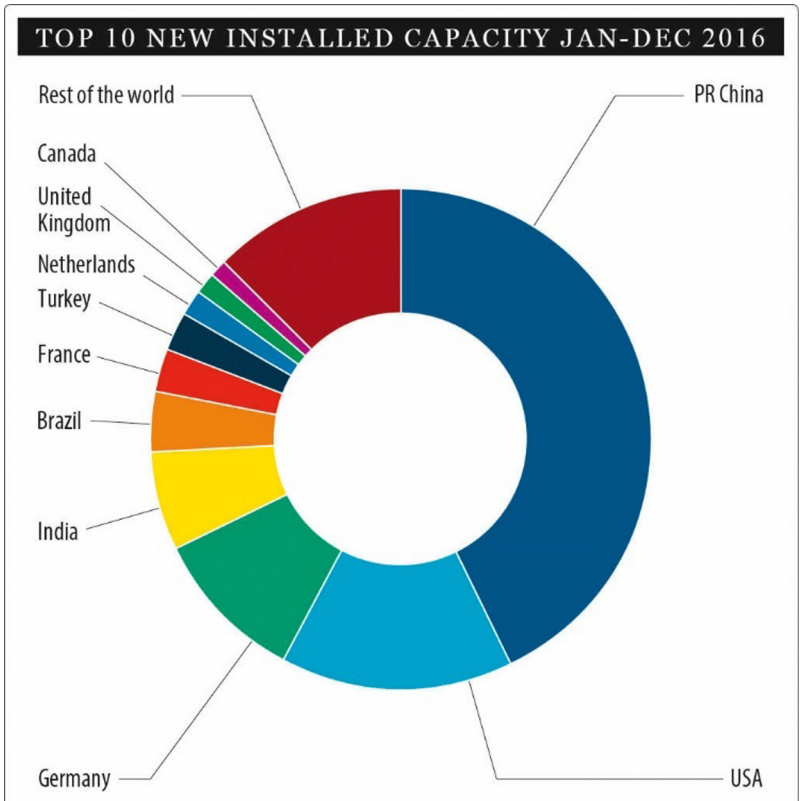

Country	MW	% Share
PR China	23,370	42.8
USA	8,203	15.0
Germany	5,443	10.0
India	3,612	6.6
Brazil*	2,014	3.7
France	1,561	2.9
Turkey	1,387	2.5
Netherlands	887	1.6
United Kingdom	736	1.3
Canada	702	1.3
Rest of the world	6,727	12.3
Total TOP 10	**47,915**	**88**
World Total	**54,642**	**100**

Source: GWEC

Fig. 2. New installed capacity for top 10 countries in 2016 [3].

Different aspects such as blade profile modification and optimization, wind turbine performance augmentation using guide vanes and shrouds, wind turbines wake interaction in wind farms, wind turbine aeroacoustics, dynamic stall, unsteady and skewed wind flow conditions, and self-starting characteristics are considered. The effect of different operating and geometrical parameters such as tip speed ratio, wind speed, solidity, blade number and blade shapes on the wind turbine performance and self-starting characteristics are reviewed. Moreover, guidelines and recommendations for turbulence modeling, spatial and temporal discretization, numerical scheme and algorithm, computational domain size are provided. Different turbulence modeling and their advantages and disadvantages will be discussed.

2. Guidelines and recommendations toward reliable and accurate CFD simulation for VAWTs

This section aims to provide guidelines and recommendations towards accurate and reliable CFD simulation of Darrieus VAWTs. Appropriate spatial and temporal discretization, numerical scheme and algorithm, computational domain size is discussed.

A crucial aspect of reliable wind turbine CFD simulation is the computational grid. High quality grid can improve the convergence rate and computational accuracy, while low quality grid may lead to meaningless results or even calculation failure. Generally, Grids are categorized into structured and unstructured grids. In structured grids, every node is uniquely identified by the indexes i, j

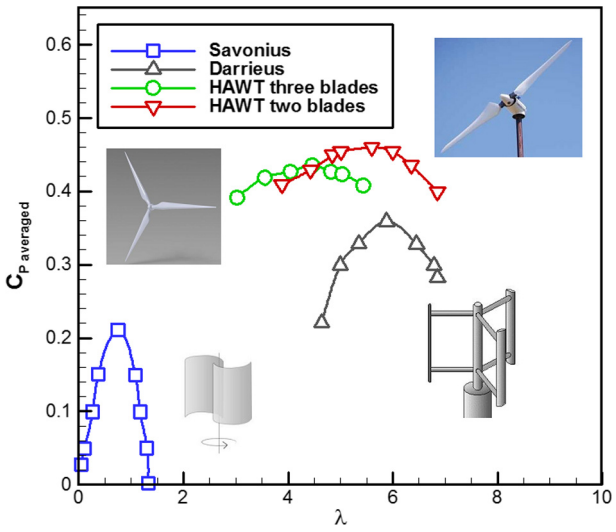

Fig. 3. Characteristic curves of $C_{p-averaged}$ as a function of λ for various wind turbines. Adapted from [9,10].

and k and the grid elements are quadrilaterals in 2D and hexahedra in 3D. On the other hand, grid points have no particular ordering in unstructured grid and neighboring grid points cannot be directly identified by their indexes. The main advantage of structured grids is due to the linear address space representation of grid point indexes. This property leads to a very quick and easy access to the neighbors of a grid node. But it is difficult to generate structured grids for complex geometries [24]. Fig. 4 depicts a structured computational grid for a Darrieus wind turbine.

The required grid resolution strongly is problem dependent. Therefore, grid sensitivity study is required to determine the appropriate grid resolution [11,26–30]. Generally, using finer grid makes the numerical results more accurate, but it also requires higher computer memory and computational cost. The optimum grid size can be determined by increasing the grid number until the mesh is sufficiently fine. Therefore, further refinement does not change the results significantly. Fig. 5 shows a computational grid independency study for three different mesh resolutions: coarse, medium and fine. As it can be seen, there is little difference in the solution between medium and fine meshes. Therefore, medium grid is the best computational grid. Zadeh et al. [29] employed the Grid Convergence Index (GCI) method to analyze the grid convergence and estimate the discretization error.

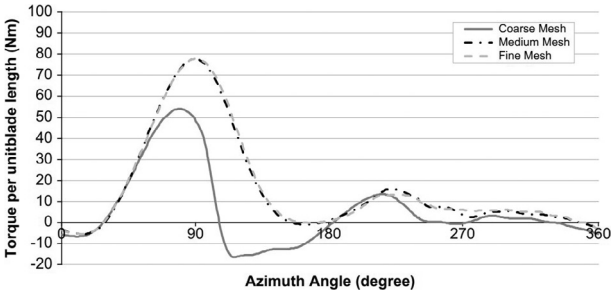

Fig. 5. Computational grid independency study [31].

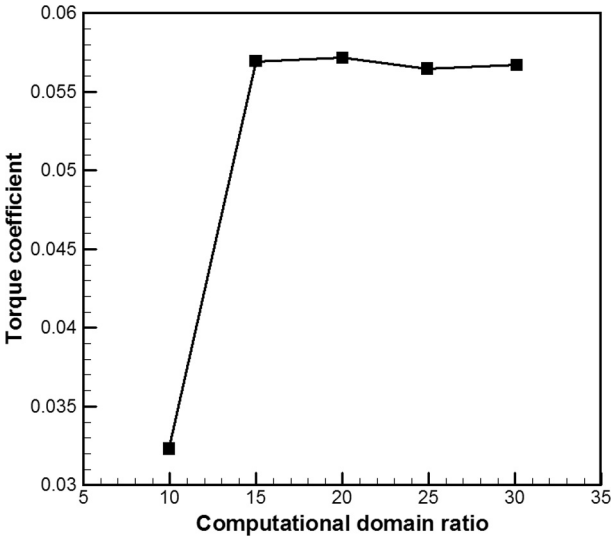

Fig. 6. Computational domain size sensitivity study [34].

It is particularly required that the grid points should be clustered near the blade and in the wake region, where the velocity gradients are high. The dimensionless wall parameter, y^+, is an important factor describing how many cell points should be located within the wall boundary layer. Wall function in every turbulence model is valid within a specific range of y^+. The y^+ should be compatible with turbulence wall function. The y^+ associated with the first cell should not be too large that the first node falls outside of the log-law layer and it should not be too small that the first node is placed in the viscous sublayer of the boundary layer [11,26–30].

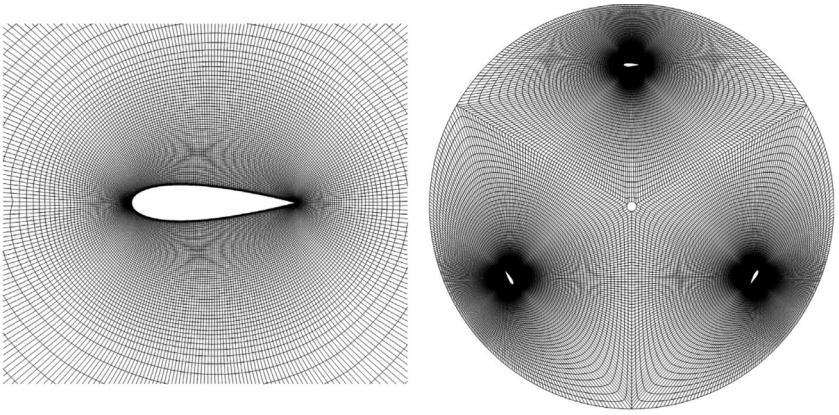

Fig. 4. Structured computational grid around blade [25].

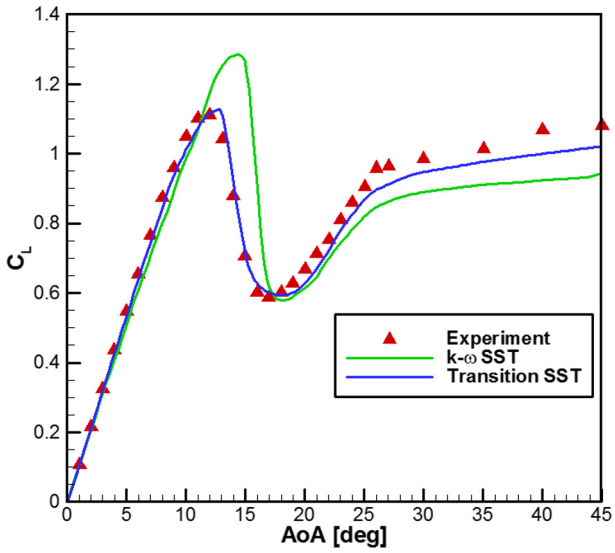

Fig. 7. Lift coefficient comparison for transition SST and $k-\omega$ *SST* turbulence models. Adapted from [32].

The Mach number for Darrieus wind turbine application is less than 0.3 ($M < 0.3$); therefore the flow can be considered incompressible and incompressible flow solvers may be employed [19]. SIMPLE (Semi-Implicit Method for Pressure Linked Equations), PISO (Pressure-Implicit with Splitting of Operators) and COUPLED pressure-velocity coupling methods were evaluated on different operating conditions by Lanzafame et al. [32]. They suggested that the best results were obtained using the PISO scheme, while SIMPLE scheme was inefficient at low tip speed ratios and COUPLED scheme was unable to predict the flow behavior around the blades.

In any CFD simulation, it is required to assess if the solution to discretized governing fluid flow equations have converged to final solution through some iterative procedures. There are several ways to check the solution convergence. One way is to check if the residuals of the iterative process for the governing equations have reached under a certain value. Monitoring an accumulating aerodynamic quantity such as lift or torque may present a constant oscillating trend. The mass conservation (balance) between inlet and outlet is normally required to be verified.

The time step should be small enough to adequately capture the small-scale turbulent eddies with high frequency especially at high rotational speed and high wind speed. Castelli et al. [33] established a simulation with an angular step of 1 degree. It is suggested that the rotational speed is gradually increased to make the simulation process less "aggressive". The computational domain size should be enough large to minimize the effects of blockage and uncertainties in the boundary conditions on the results and correctly reproduce the wake effect and flow around the rotor. On the other hand, it should not be too large to not uselessly increase elements number and computational time [32]. Chen et al. [34] carried out sensitivity study of computation domain size. It was shown that the torque is relatively constant when the ratio of computational domain to rotor diameter is larger than 15 (see Fig. 6). The computational domain should be extended enough (14 diameters) downwind with respect to the rotor to allow a full development of the wake [35,36]. Mohamed [37] suggested the computational domain ratio of 20. Rezaeiha [38] used a computational domain with a distance from the turbine center to the domain inlet and outlet of 10D each, a domain width of 20D and a diameter of the rotating core of 1.5D.

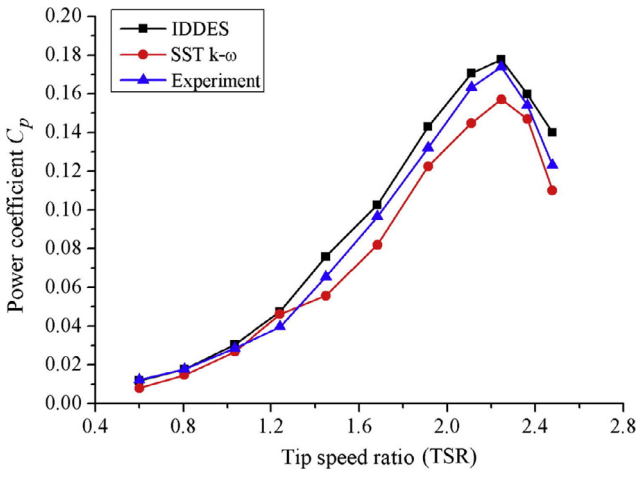

Fig. 8. Comparison of power coefficient at different tip speed ratios for IDDES and $k-\omega$ *SST* turbulence models [53].

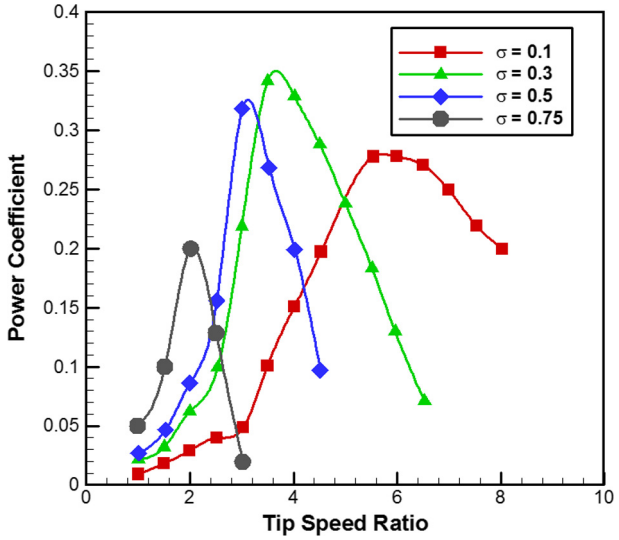

Fig. 9. Effects of solidity on the wind turbine performance. Adapted from [54].

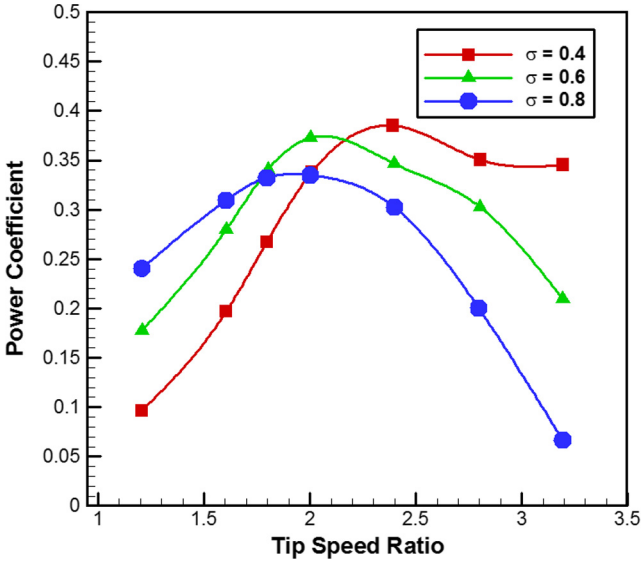

Fig. 10. Solidity effects on wind turbine performance. Adapted from [55].

3. Applications of different turbulence models for Darrieus VAWTs

This section is devoted to review different approaches to model turbulent flows around Darrieus VAWTs. Advantages and disadvantages of several intensively used turbulence models such as $k-\varepsilon$, $k-\omega(SST)$, SST transition, Large Eddy Simulation (LES), and hybrid RANS-LES are discussed.

3.1. The $k-\varepsilon$ turbulence model

The $k-\varepsilon$ turbulence model computes the eddy viscosity in the Reynolds averaged Navier-Stokes (RANS) equations by solving two transport equations for turbulent kinetic energy, k, and turbulent dissipation rate, ε. This model is numerically stable and robust. Therefore, it is popular for a wide range of turbulent flows in industrial flow and heat transfer simulations. This section presents the eddy viscosity type models including the standard, Renormalization Group (RNG), and realizable $k-\varepsilon$ turbulence models. All models have similar transport equations for turbulent kinetic energy and turbulent dissipation rate. The major differences among the eddy viscosity models are the turbulent viscosity calculation method, generation and destruction terms in the ε equation, and the turbulent Prandtl numbers governing the turbulent diffusion of k and ε.

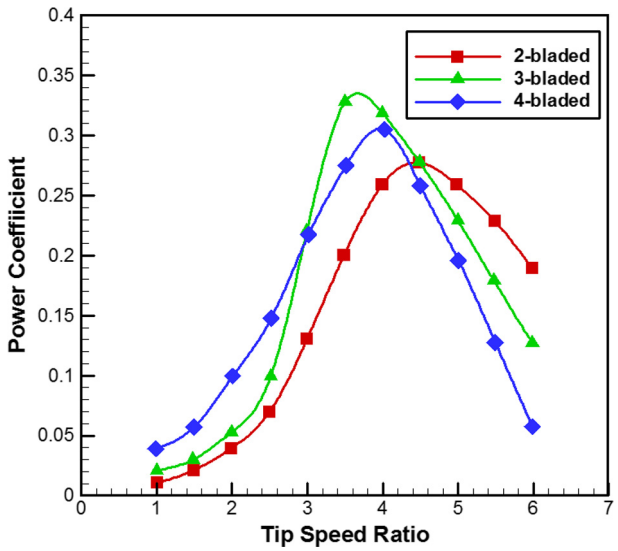

Fig. 11. Effects of blade number on the wind turbine performance. Adapted from [54].

The $k-\varepsilon$ turbulence model determines the turbulent length and time scale by solving two transport equations for the k and ε. The $k-\varepsilon$ turbulence model is a semi-empirical model and the derivation of the model equations relies on phenomenological considerations and empiricism. The $k-\varepsilon$ turbulence model assumes that the flow is fully turbulent and neglects the effects of molecular viscosity.

The RNG $k-\varepsilon$ turbulence model [39] was derived using a statistical technique called "renormalization group" (RNG) theory [40]. This model has several modifications such as considering the effects of rotation on the eddy viscosity, an additional term in ε equation for rapidly strained flows, and employing an analytical formula for turbulent Prandtl numbers instead of constant values in the standard $k-\varepsilon$ turbulence model. Therefore, the RNG $k-\varepsilon$ turbulence model due to these features is more accurate and reliable for a wider range of turbulence flows compared to standard $k-\varepsilon$ turbulence model.

The realizable $k-\varepsilon$ turbulence model [41] is usually recommended for rotating bodies [37]. The C_μ in this turbulence model is expressed as a function of mean flow and turbulence properties, in contrast with the standard model which is assumed to be constant. This model leads to improved results for swirling flows and some flows involving separation.

3.2. The $k-\omega(SST)$ turbulence model

The $k-\omega(SST)$ (shear stress transport) turbulence model is a combination of superior elements of $k-\omega$ and $k-\varepsilon$ turbulence models. It utilizes the $k-\omega$ turbulence model in the inner part

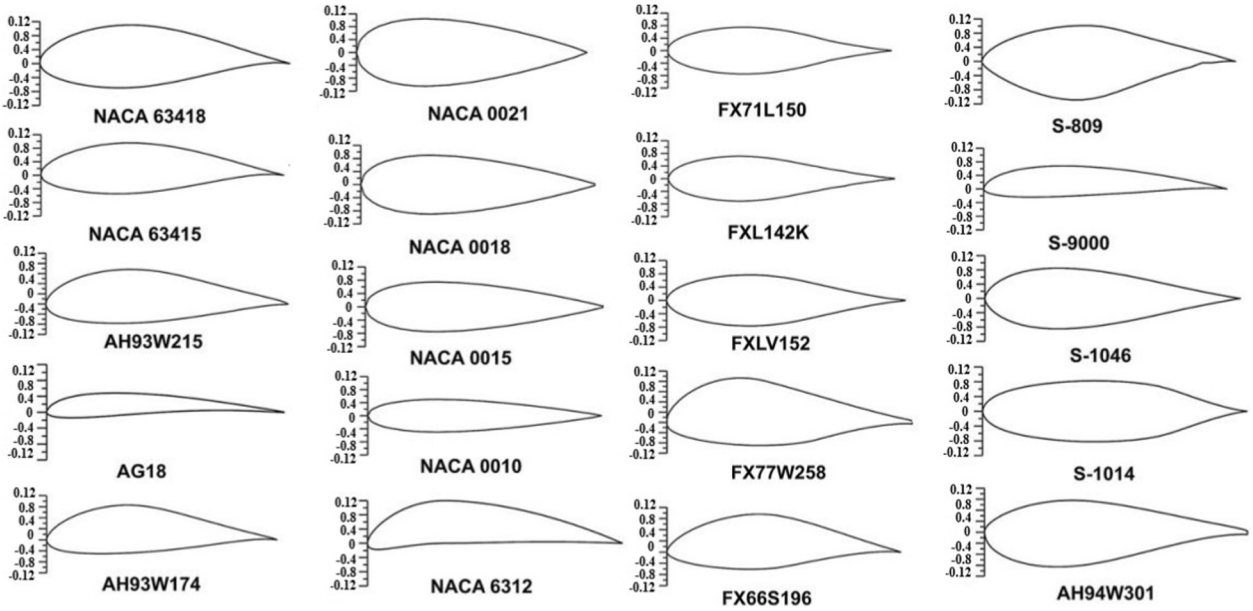

Fig. 12. Different symmetric and non-symmetric airfoils studied by [37].

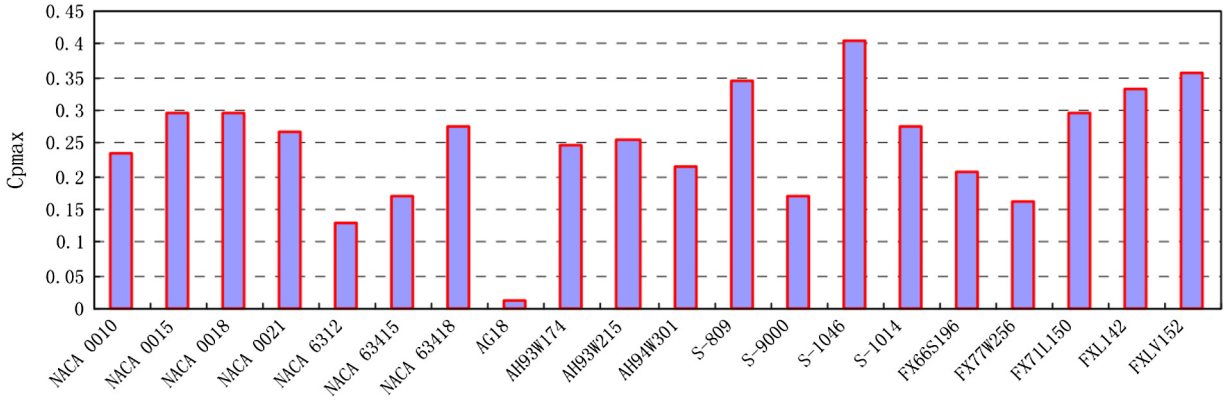

Fig. 13. Maximum power coefficient for different symmetric and non-symmetric airfoils studied by [37]. Adapted from [19].

of the boundary layer and gradually switches to the standard $k-\varepsilon$ turbulence model in the wake region of the boundary layer and free shear layers [42]. The transition between these two models is based on a blending function. This blending function is one in the sublayer and logarithmic region of boundary layer and gradually switches to zero in the wake region and free shear layers. The other superiority of $k-\omega(SST)$ turbulence model is that the eddy viscosity formulation is modified to take into account the effect of turbulent shear stress transportation. This turbulent shear stress transportation is important to predict severe adverse pressure gradient flows [43]. The $k-\omega(SST)$ turbulence model was employed in several studies such as [44–46].

3.3. The SST transition turbulence model

The SST transition turbulence model is based on the coupling of the $k-\omega(SST)$ transport equations with two other transport equations for the intermittency and the transition momentum thickness Reynolds number. The SST transition turbulence model leads to more accurate results compared to the classical fully turbulent models. While the fully turbulent RANS models lead to an overestimation of the generated power, transition model is capable to predict flow separation phenomena [32] (see Fig. 7). Several studies used SST transition turbulence model to investigate flow characteristics around VAWTs such as [14,32,45,47].

3.4. The large eddy simulation

The Large Eddy Simulation (LES) is based on a scale separation. The large scales which contain the most energy and transport the flow properties are resolved, but the small scales which behave in universal way are simply modeled. LES is accurate, but it is rather computationally expensive. Large eddy simulation of VAWTs can be found in [48–51].

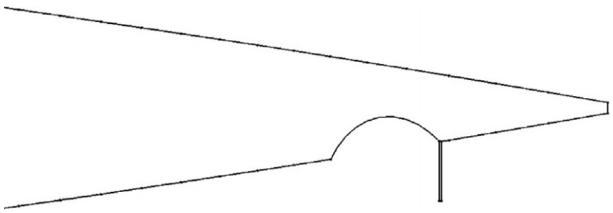

Fig. 14. NACA-0015 having Gurney flap with inward dimple on the lower surface near the trailing edge [66].

3.5. The hybrid RANS-LES turbulence model

The hybrid RANS-LES turbulence model is a blending technique between the statistical RANS and LES method. The basic principle in hybrid technique is to solve the boundary layer with RANS, whereas LES is employed for the external flow and separation regions. This method overcomes the excessive computational demands of LES and has better accuracy compared to the RANS [52]. The hybrid RANS-LES turbulence model was employed by several authors in wind turbine applications [47,53]. Fig. 8 shows the comparison of power coefficient at different tip speed ratios for IDDES and $k-\omega$ *SST* turbulence models [53].

4. Effects of different geometrical and operating conditions on the performance of Darrieus VAWTs

4.1. The effects of solidity

The power extraction performance of Darrieus VAWTs depends on the different parameters such as rotor diameter, chord length, solidity, tip speed ratio, blade profile, spanwise height, installation angle, and blade number. This section reviews the CFD studies that investigated the effects of these parameters on the wind turbine performance.

Solidity is defined based on the number of blades, *N*, chord length, *c*, and rotor radius, *R*, as follow:

$$\sigma = \frac{Nc}{R} \tag{1}$$

Sabaeifard et al. [54] studied the effects of solidity on the wind turbine performance. Increasing solidity to range of 0.3–0.5 improved turbine performance. However, above this range of solidity, the power coefficient decreased significantly and the curve exhibited sharper peaks. Fig. 9 shows the power coefficient for different solidities.

Lee and Lim [55] investigated the effect of various parameters such as chord length, helical angle, pitch angle, and rotor diameter on the wind turbine performance. As Fig. 10 shows, the longer chord length and smaller rotor diameter (higher solidity) increased the power performance in the range of low tip speed ratios. But, in the higher tip speed ratios, lower solidity rotors performed better. The observations indicated that the dominant power affecting blades is lift at low tip speed ratios. However, as the tip speed ratio increases, the drag is the most dominant parameter causing variations in the wind turbine performance. In the case of the lift, the long-chord length rotor displays a higher power coefficient. On the contrary, when the drag is regarded as the dominant parame-

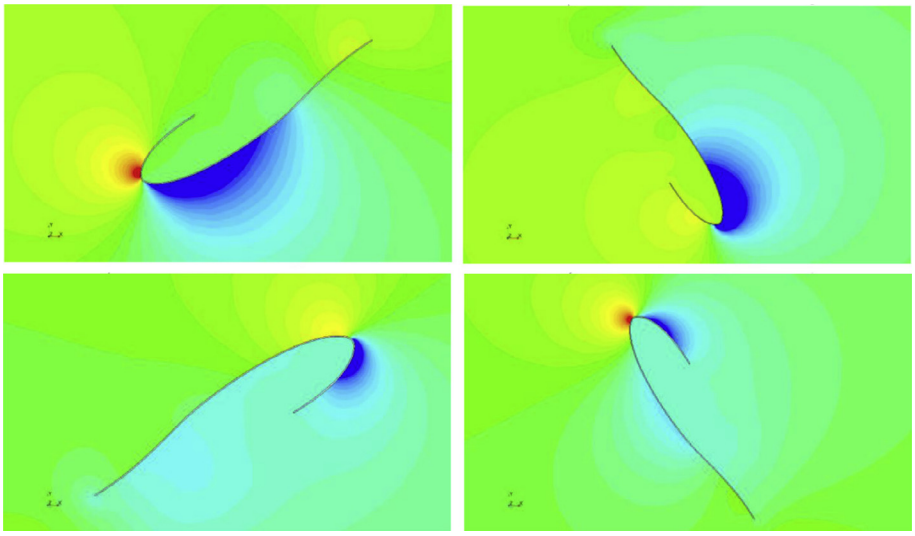

Fig. 15. Pressure field around J-shaped blade for different times [68].

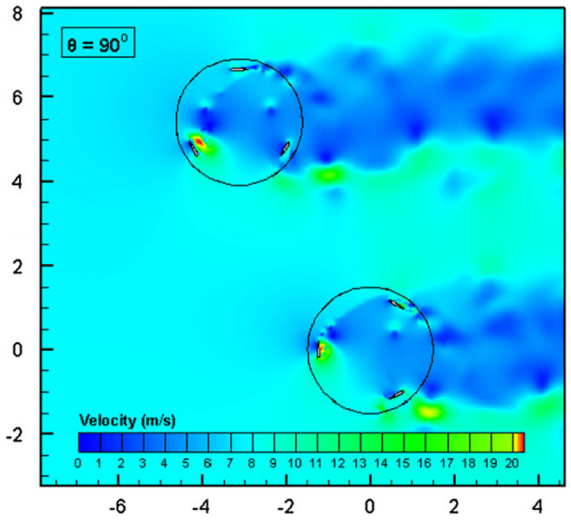

Fig. 16. Velocity contour around the two turbines [75].

ter, the long-chord length rotor displays a lower performance because it encounters stronger resistance.

Gang and Kau [56] investigated the effects of blade installation angle and chord length. The power coefficient in the best solidity was increased by 15%. The rotor power coefficient first increased then declined as the solidity increased. Also, the operating range kept declining by the solidity increase. Another study [57] showed that the best performing turbine has solidity around $\sigma = 0.2$. The low solidity is recommended for H-Darrieus wind turbine to obtain wider operating ranges [37]. Both the torque and power coefficients are shifted left with increasing the solidity due to the wake effect increases in narrow passages between blades and the chance of the earlier stalling. Decreasing the instantaneous torque and power coefficient occur with increasing the solidity.

Sensitivity study to the blade number can be found in the works done by [54,57,58]. The torque variation reduces during the revolution of a VAWT by increasing the blade number. Fig. 11 shows the power coefficient variation for different blade number. Larger number of blades allowed to reach the maximum power coefficient for lower angular velocity. On the contrary, lower number of blades led to higher performance for higher tip speed ratios. The best power performance occurs when the rotor has 3 blades.

4.2. The effects of airfoil shape

Mohamed et al. [59] investigated different blade airfoil sections and blade pitch angles. They found that the LS (1)-0413 airfoil section increased the power coefficient around 10% compared to NACA 0018 airfoil section. Also, they reported that the airfoil section of NACA 63-415 introduced wider operating range. The effect of pitch angle variation was investigated from $-10°$ to $10°$ compared with zero pitch angle. Surprisingly, the zero-pitch angle led to the best performance. Mohamed [37] studied 20 different symmetrical and unsymmetrical airfoil shapes including NACA 00XX, NACA 63XXX, S-series, A-series, and FX-series as shown in Fig. 12 to maximize the wind turbine performance. The maximum power gained for different airfoil shapes is shown in Fig. 13. The S-1046 airfoil section led to a 26.83% increase in maximum power output coefficient compared to the standard symmetrical NACA airfoils. The operating range was extended up to $\lambda = 10$ using small solidity ($\sigma = 0.1$). The operating range (tip speed ratio range) for symmetrical airfoils was observed wider than non-symmetrical airfoils because stall was delayed using symmetrical airfoils.

The study of the blade thickness and camber effects on the wind turbine performance showed that the thicker airfoils tend to per-

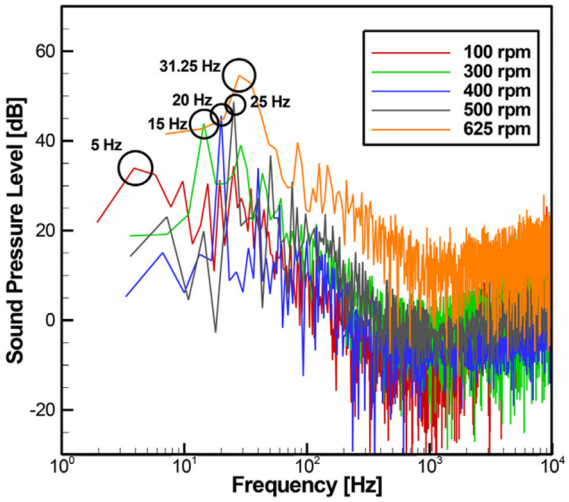

Fig. 17. Tip speed ratio effects on the noise generation of H-Darrieus wind turbine.

form better for high solidity ratio. This is mainly due to the better inheriting stall characteristics of thicker airfoils. It was found that the symmetrical airfoil sections had a slightly better performance at tip-speed ratios corresponding to highest power coefficient values without a noticeable effect on the self-starting of the VAWT [49].

Bausas and Danao [60] studied the aerodynamics of a camber-bladed VAWT in unsteady free stream under fluctuating wind condition. Camber along the rotation path marginally improves the overall performance of VAWT. Sengupta et al. [61] studied starting characteristics, dynamic performance, and flow physics of high solidity symmetrical and unsymmetrical VAWT blades. They concluded that using unsymmetrical or cambered blades with high solidity instead of symmetrical blades can improve the wind turbine starting performance along with its power coefficient.

Castelli and Benini [62] studied the effects of phase shift angle between lower and upper blade sections. The average torque did not change substantially for low phase shift angle but showed a remarkable decrease for high values of phase shift angle between upper and lower blade sections. Investigation of pressure variation in spanwise direction of Darrieus VAWTs in unsteady wind condition showed that the momentum amount is the largest at the blade center height and the smallest at the blade tip [63]. Li et al. [64] evaluated the aerodynamic forces and inertial contributions to rotor blade deformation. They predicted the aerodynamic performance of straight-bladed VAWT in the spanwise direction. The fluid force decreased with the increase of spanwise positions excluding the position of support structure.

5. Different application of CFD in Darrieus VAWTs

5.1. Modification and new design of Darrieus VAWTs

This section addresses the optimization and modification in Darrieus VAWTs design to improve performance. Bedon et al. [65] employed an optimization method to develop a new airfoil shape to increase the aerodynamic performance. Chen et al. [34] optimized the NACA 4-digit airfoil family by parameterization. Ismail and Vijayaraghavan [66] modified the blade profile by combination of inward semi-circular dimple and Gurney flap at the lower surface of the NACA-0015 airfoil. The optimized shape of the modified airfoil is shown to improve the aerodynamics of the wind turbine blade. The average tangential force increased by approximately 35% by utilizing an optimized combination of Gurney flap and semi-circular inward dimple. A schematic of their design is shown in Fig. 14.

Jafaryar et al. [67] optimized the asymmetric blades. Their results showed that the optimum shape of the airfoil is very similar to symmetric blades. The starting torque improvement using J-shaped blade profile was proposed by Zamani et al. [68,69]. The J-shaped profile was designed by eliminating the pressure side of airfoil from the maximum thickness toward the trailing edge. This design can benefit from the lift and drag forces simultaneously. This combined force can help the turbine possesses faster operation at low wind speeds. Thereby resulting in the termination of self-starting problem and improving the power coefficient, especially at low and moderate tip speed ratios. These improvements can be attributed to the inherent geometry of J-shaped profile through which the generated vorticities are trapped inside the blade and released behind the rotor. Fig. 15 shows the contour of pressure for this type of wind turbine at different azimuth angles.

5.2. Wind farm arrangements of Darrieus VAWTs

A principle challenge in wind energy field is that wind is more diffuse. Therefore, a substantial land resource is required to extract perceptible amount of energy. The power density of wind farms is defined as the power extracted per unit land area. HAWTs wind farms require significant land resources to isolate each wind turbine from the aerodynamic interaction with adjacent turbine wakes. This aerodynamic constrain limits the power density of typ-

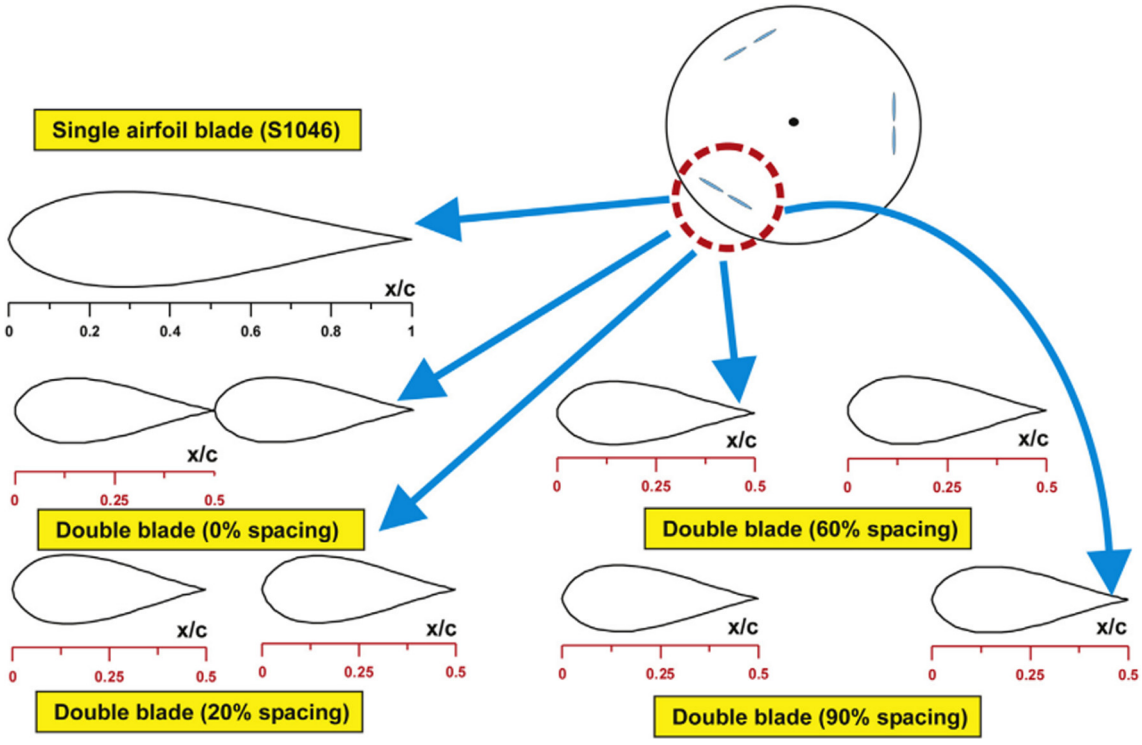

Fig. 18. Different configurations of the double-airfoil blade [81].

ical HAWTs wind farms between 2 and 3 W/m^2. VAWTs have the potential to acquire higher power densities and this possibility is because the VAWTs swept area can be apportioned unequally between its breadth -which determines the wind turbine footprint size- and height, on the other hand, the HAWT circular sweep dictate that the breadth and height of the rotor swept area should be identical. Therefore, the power density of H-rotor VAWTs wind farms can be improved to 30 W/m^2 by arranging wind turbines in layouts that enables them to extract energy from adjacent turbine wakes [70]. The grouping of turbines in wind farms results in distributed flows behind rotors with reduced wind speeds. The power losses due to wind turbine wakes can be of the order of 10–20% of the total power output of large wind farms. Therefore, the wind turbines arrangement in wind farm is important to enhance the wind farm power generation. A detailed knowledge of the flows and turbulence structures within wakes is necessary to optimize the wind farm turbine layout [71–73]. Therefore, this section focuses on the Darrieus wind turbine arrangements in the wind farms.

Giorgetti et al. [74] studied the aerodynamic interaction between two medium-solidity Darrieus VAWTs positioned in close proximity. The behavior of counter-rotating and co-rotating arrangements was analyzed at different distances between rotor axis. 10% power production improvement was observed compared to the isolated turbine regardless of the rotation direction. The accelerated free-stream flow between the turbines causes power extraction enhancement. The results of a sensitivity analysis to wind direction suggested that closely spaced multi-rotor arrangement should be only used in sites with strong prevailing wind directions.

The other study showed that the dual turbine system operated at the optimal combination can enlarge the power performance by 9.97% [75] (see Fig. 16).

A pair of counter-rotating VAWTs in various gaps between the two turbines, tip speed ratios and wind directions were analyzed to identify the local flow mechanisms contributing to enhanced power generation compared to the isolated one. For two turbines arrayed side-by-side with respect to the incoming wind, the power enhancement can be due to [76]:

1. Change of lateral velocity in the upwind path due to the presence of the neighboring turbine, making the direction of local flow approaching the blade more favorable to generate lift and torque.
2. Contraction of the wake in the downwind path making a larger momentum flux available for power generation in the downwind path.

Chowdhury et al. [77] investigated the adjacent wake effects of VAWTs and determined the suitable flow recovery for optimal placement of subsequent turbines. The wake interference is minimal at around 5D of turbine downstream and there is an adequate flow recovery in this location.

Lam and Peng [47] studied the near and far wakes characteristics. In the near wake, the velocity suffered a drastic deficit of about 85%. In the far wake, major velocity recovery occurred with the average streamwise velocity reaching approximately 75% at 10D.

5.3. Aerodynamic noise pollution of H-Darrieus wind turbines

Aerodynamic noise from Darrieus wind turbines may cause annoyance for people living near the turbines. Noise emitted from an operating wind turbine can be divided into mechanical noise and aerodynamic noise. Mechanical noise originates from different machinery components, such as the generator and the gearbox. Aerodynamic noise is radiated from the blades and is mainly associated with the interaction of turbulence with the blade surface. Machinery noise can be reduced efficiently by well-known engineering methods [78], whereas reduction of aerodynamic noises still represents a problem, and aerodynamic noise is the dominating noise mechanism. Therefore, it is important to identify and predict the most important noise sources. The aerodynamic noise source can be classified into discrete frequency (tonal) noise and broadband noise in character.

The early numerical studies [79] used discrete vortex method to compute the aerodynamic noise generated by wind turbines. In the recent years, CFD is more common to study different generation mechanism noises. Ghasemian and Nejat [51] employed incompressible Large Eddy Simulations and Ffowcs Williams and Hawkings (FW-H) acoustic analogy formulation to predict the aerodynamic noise generation by H-Darrieus wind turbine at different tip speed ratios. The broadband noises of the turbulent boundary layers and the tonal noises due to the blade passing frequency were analyzed. Fig. 17 depicts the effects of rotational speed on the sound pressure level. Every rotational speed has a distinct tonal peak corresponded to the blade rotation frequency.

Mohamed [80] investigated the aerodynamic noise of the Darrieus VAWT with different blade shapes, tip speed ratios and solidities using URANS and FW-H. Four different airfoils S-1046, NACA 0018, NACA 63418 and FXLV152 were studied. Results showed that S-1046 airfoil which has the best aerodynamic performance has less noise generation. Wind turbine is noisier at the higher solidities and higher tip speed ratios. The noise emission reduced by 7.6 dB when the solidity decreased from 0.25 to 0.1. An innovative design proposed by Mohamed [81] to reduce the noise generation in VAWTs. In his design, every blade was constructed by two airfoils (see Fig. 18). His results showed that the 60% spacing is the best configuration of the double-airfoil from the noise reduction point of view. The new configuration reduced the average sound level by 56.55%. Nevertheless, the optimum design decreased the power coefficient by 6.8%.

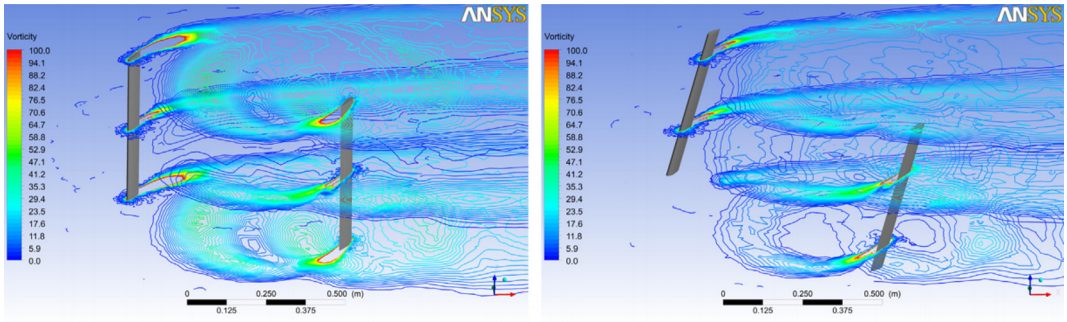

Fig. 19. Vorticity contours for the upright and tilted configurations [87].

5.4. Wind turbine performance in fluctuating and skewed wind conditions

Most of CFD studies assume an unchanged and steady incoming wind flow conditions, but in reality due to the presence of buildings and other adjacent obstructions in the urban environments, wind is normally skewed, fluctuating, and tilted [82,83]. This section focuses on the unsteady, fluctuating and inclined incoming wind flows. Several authors studied the VAWTs performance in unsteady and fluctuation incoming flows [25,60,84,85]. Danao et al. [25] concluded that the overall performance can be slightly improved if the mean tip speed ratio is just above the tip speed ratio of the steady performance maximum, the amplitude of fluctuation is small (<10%), and the frequency of fluctuation is high (>1 Hz). Bhargav et al. [84] investigated the effect of variation of fluctuation amplitude and frequency of incoming free stream wind. As fluctuation amplitude increased from 10% to 50%, cycle averaged power coefficient continuously increased from 0.284 to 0.329. Increase in fluctuation frequency increased the power coefficient till $f = 1$ Hz, further increase in frequency resulted in marginal decrease in power coefficient. Wekesa et al. [85] also concluded that the highest frequency of fluctuation with energy content in unsteady wind condition is $f \approx 1$ Hz. Unsteady wind imposed a detrimental effect to VAWT performance [60].

The distortion of the flow by buildings within the urban environment causes the VAWT operate in oblique flow and the wind is non-perpendicular to the axis of rotation of the wind turbine. The VAWT in oblique flow is equivalent to VAWT working in tilted condition [82]. In contrast to HAWT, VAWT is known to perform positively in some tilted conditions. Chowdhury [86] studied the upright and tilted configurations. Their results showed that the torque produced by the tilted condition was higher than the upright configuration. The flow field visualization showed the wake of tilted configuration would proceed downstream in tilted manner and the wake stream shifts downward. The VAWT performance increment in skewed flow was studied by Orlandi et al. [87]. The power gain in the skewed flows was obtained during the downwind phase of the revolution. This gain is due to the downwind part of the rotor being less disturbed by the wake generated by the blades in the upwind part as is shown in Fig. 19. Bedon et al. [44] carried out CFD simulations for tilted Darrieus turbine. A sensible decrease in the power production was observed for increasing tilt angles. This decrease in power can be due to the direction of tilt angle which is towards the incoming wind instead of being downward.

The performance of VAWT under accelerating and decelerating flows was studied by Shahzad et al. [88]. Siddiqui et al. [89] investigated the effect of turbulence intensity on the performance of an offshore wind turbine. Due to the increase in turbulence intensity level from 5% to 25% the performance of wind turbine decreases by almost 23–42% compared to no turbulence in the incoming wind field. Lei et al. [90] investigated the impact of pitch motion of a floating vertical axis wind turbine with different periods and amplitudes. The pitch motion can improve the power output of the VAWTs and enlarge the variation ranges of aerodynamic force coefficient. The additional velocity induced by pitching is the primary factor that affects the instantaneous aerodynamic forces and sweep area and tilt angle are the minor factors. The power coefficients of the wind turbine increased with the growth of pitching amplitudes and the pitching periods reduction. The tip blade vortices become stronger in pitch motion, which is induced by the stronger blade-wake interaction.

5.5. Wind turbine performance augmentation using guide vanes

Using the guide vane is an appropriate strategy to increase the wind turbines performance and improve their self-starting

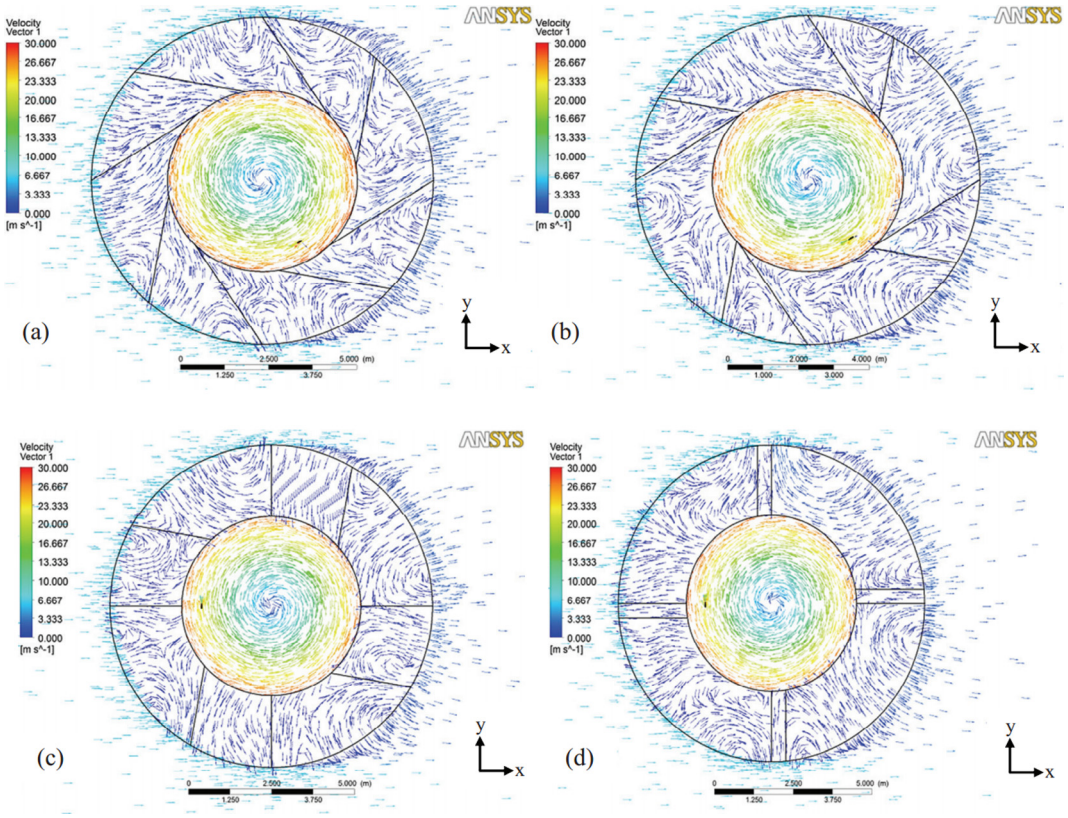

Fig. 20. Velocity vector field for different omni-direction-guide-vane configuration [92].

capability especially at the lower wind speeds. Several CFD studies [31,91–94] were devoted to the shrouded H-Darrieus wind turbines.

The omni-direction-guide-vane (ODGV) surrounds the VAWT to increase the on-coming wind speed, change the flow angle for better angle of attack of the wind turbine blades, and increase the rotational speed and working hour of the wind turbine. The working concept of the ODGV is to minimize the negative torque zone and reduce turbulence and rotational speed fluctuations [91]. Nobile et al. [31] carried out CFD simulations of an open and augmented Darrieus straight-bladed VAWT. Their results indicated that the introduction of an omnidirectional stator around the same rotor has the potential to increase the average power and torque coefficients by about 30–35%. Lim et al. [92] optimized the ODGV design parameters such as guide vanes angles and the ratio of diameter to distance between two guide vanes in order to maximize the wind turbine performance. Fig. 20 shows velocity vector field for different omni-direction-guide-vane configurations [92]. The omni-direction-guide-vane angles effects also was evaluated in the recent work by Shahizare et al. [93]. Zanforlin and Letizia [94] improved the performance of wind turbines in the urban environment by integrating the action of a diffuser with the aerodynamics of the rooftops. The combination of a dual-pitched roof and a diffuser-shaped wall allowed to obtain a power enhancement of 40–50%.

5.6. Self-starting characteristics of Darrieus wind turbines

The inherent start-up issues associated with VAWTs limit their installation especially in environments with low wind speed. Therefore, it is crucial to study the self-starting behavior of this type of wind turbine. Several studies [14,95,96] utilized CFD to study the self-starting characteristics of H-Darrieus wind turbines. To consider the self-starting characteristics, the rotor is left free to accelerate based on the torque experienced over time and the instantaneous rotational speed at each time step is computed based on the Newton's second law and according to the instantaneous aerodynamic and mechanical forces. This approach is in contrast with the conventional approach which a constant angular velocity is specified to the rotor. The start-up capability of H-Darrieus is influenced by many various factors such as blade profile, Reynolds number, secondary flow, three-dimensional aerodynamic effects and finite aspect-ratio of the blades. Rossetti and Pavesi [95] applied different approaches to describe the self-starting behavior of H-Darrieus wind turbines. The BEM model suffers of the absence of well documented airfoil characterization of aerodynamic profiles for a very low Reynolds number. Therefore, this model shows remarkable limitation to describe the self-starting behavior. The 2D CFD simulation allowed to highlight the unsteady features of the flow field and the presence of a complex vortices pattern which interact with the blade. The comparison between 2D and 3D data demonstrated the importance of 3D effects such as secondary flows and tip effects on the self-starting behavior. These 3D effects were proved to have a positive effect on the start-up characteristics. Asr et al. [96] evaluated the effects of several geometric attributes such as symmetric and cambered airfoils of different thickness with a wide range of pitch angles on the starting characteristics. Arab Golarche et al. [14] investigated the effects of the rotor moment of inertia on the start-up characteristics of the Darrieus wind turbine. As the rotor inertia increases, it takes a longer time for the turbine to reach its final velocity. In other hand, as the rotor inertia decreases, the oscillations amplitude of the turbine rotational velocity increases.

6. Conclusion

The current review paper highlighted different aspects of Computational Fluid Dynamic simulation of Darrieus VAWTs such as blade profile modification and optimization, wind turbine performance augmentation using guide vanes and shrouds, wind turbines wake interaction in wind farms, wind turbine aeroacoustics, dynamic stall, unsteady and skewed wind flow conditions, and self-starting characteristics. The effect of different operating and geometrical parameters such as tip speed ratio, wind speed, solidity, blade number and blade shapes on the wind turbine performance and self-starting characteristics were reviewed. The principle conclusions can be summarized as follows:

- The longer chord length and smaller rotor diameter (higher solidity) increases the power performance for low tip speed ratios. But, in the higher tip speed ratios, lower solidity rotors perform better. Also, the operating range keeps declining by the solidity increase. The power coefficient is shifted left with increasing the solidity due to the wake effect increases in narrow passages between blades and the chance of the earlier stalling.
- The power variation reduces by increasing the blade number. Larger number of blades allows the maximum power coefficient reaches at lower angular velocities. On the contrary, lower number of blades leads to higher performance for higher tip speed ratios.
- The grouping of wind turbines in wind farms results in distributed flows behind rotors with reduced wind speeds. Therefore, the wind farm arrangement can enhance the wind turbine power generation. This power enhancement can be due to change of lateral velocity in the upwind path due to the presence of the neighboring turbine, and making the direction of local flow approaching the blade more favorable to generate lift and torque.
- The aerodynamic noise generated by Darrieus wind turbines can be classified into the discrete frequency noises due to aerodynamic forces and the broadband noises related to the turbulent structures in the wake behind the wind turbine. The amplitude of generated noise increases by tip speed ratio and solidity. Aerodynamic noise spectrum at every rotational speed has a distinct tonal peak corresponded to the blade rotation frequency.
- Using the guide vane is an appropriate strategy to increase the wind turbines performance and improve their self-starting capability especially at the lower wind speeds. The guide vane increase the on-coming wind speed, change the flow angle for better angle of attack of the wind turbine blades, minimize the negative torque, and increase the rotational speed and working hour of the wind turbine.
- The incoming flow is normally skewed, fluctuating, and tilted due to presence of buildings and other adjacent obstructions in the urban environments. This distortion of the flow causes that the VAWTs operate in oblique flow and the wind is non-perpendicular to the axis of rotation of the wind turbine. VAWTs can perform positively in some tilted conditions. Because the downwind part of the rotor being less disturbed by the wake generated by the blades in the upwind part.

References

[1] Ghasemian M, Nejat A. Aerodynamic noise prediction of a horizontal Axis wind turbine using improved delayed detached eddy simulation and acoustic analogy. Energy Convers Manage 2015;99:210–20. http://dx.doi.org/10.1016/j.enconman.2015.04.011.

[2] Ashrafi ZN, Ghaderi M, Sedaghat A. Parametric study on off-design aerodynamic performance of a horizontal axis wind turbine blade and proposed pitch control. Energy Convers Manage 2015;93:349–56. http://dx.doi.org/10.1016/j.enconman.2015.01.048.

[3] GWEC. Global Wind Report – Annual Market Update 2016, 2017 <http://www.gwec.net/publications/global-wind-report-2/global-wind-report-2016/>.

[4] Wang Y, Sun X, Dong X, Zhu B, Huang D, Zheng Z. Numerical investigation on aerodynamic performance of a novel vertical axis wind turbine with adaptive blades. Energy Convers Manage 2016;108:275–86. http://dx.doi.org/10.1016/j.enconman.2015.11.003.

[5] Sharma S, Sharma RK. CFD investigation to quantify the effect of layered multiple miniature blades on the performance of Savonius rotor. Energy Convers Manage 2017;144:275–85. http://dx.doi.org/10.1016/j.enconman.2017.04.059.

[6] Bianchini A, Ferrara G, Ferrari L. Design guidelines for H-Darrieus wind turbines: optimization of the annual energy yield. Energy Convers Manage 2015;89:690–707. http://dx.doi.org/10.1016/j.enconman.2014.10.038.

[7] Sharma S, Sharma RK. Performance improvement of Savonius rotor using multiple quarter blades – a CFD investigation. Energy Convers Manage 2016;127:43–54. http://dx.doi.org/10.1016/j.enconman.2016.08.087.

[8] Roy S, Saha UK. Review on the numerical investigations into the design and development of Savonius wind rotors. Renew Sustain Energy Rev 2013;24:73–83. http://dx.doi.org/10.1016/j.rser.2013.03.060.

[9] Akwa JV, Vielmo HA, Petry AP. A review on the performance of Savonius wind turbines. Renew Sustain Energy Rev 2012;16:3054–64. http://dx.doi.org/10.1016/j.rser.2012.02.056.

[10] Eldridge FR. Wind machines. 2nd ed. Van Nostrand Reinhold Co.; 1980.

[11] Daróczy L, Janiga G, Petrasch K, Webner M, Thévenin D. Comparative analysis of turbulence models for the aerodynamic simulation of H-Darrieus rotors. Energy 2015;90:680–90. http://dx.doi.org/10.1016/j.energy.2015.07.102.

[12] Wang LB, Zhang L, Zeng ND. A potential flow 2-D vortex panel model: applications to vertical axis straight blade tidal turbine. Energy Convers Manage 2007;48:454–61. http://dx.doi.org/10.1016/j.enconman.2006.06.017.

[13] Beri H, Yao Y. Double multiple streamtube model and numerical analysis of vertical axis wind turbine. Energy Power Eng 2011;3:262–70. http://dx.doi.org/10.4236/epe.2011.33033.

[14] Arab Golarche A, Javadi Malabad SM, Anbarsoozb M. A numerical study on the aerodynamic performance and the self-starting characteristics of a Darrieus wind turbine considering its moment of inertia. J Renew Energy 2017. http://dx.doi.org/10.1016/j.renene.2017.02.013.

[15] Islam M, Ting DSK, Fartaj A. Aerodynamic models for Darrieus-type straight-bladed vertical axis wind turbines. Renew Sustain Energy Rev 2008;12:1087–109. http://dx.doi.org/10.1016/j.rser.2006.10.023.

[16] Kang C, Liu H, Yang X. Review of fluid dynamics aspects of Savonius-rotor-based vertical-axis wind rotors. Renew Sustain Energy Rev 2014;33:499–508. http://dx.doi.org/10.1016/j.rser.2014.02.011.

[17] Chen J, Yang H, Yang M, Xu H, Hu Z. A comprehensive review of the theoretical approaches for the airfoil design of lift-type vertical axis wind turbine. Renew Sustain Energy Rev 2015;51:1709–20. http://dx.doi.org/10.1016/j.rser.2015.07.065.

[18] Tummala A, Velamati RK, Sinha DK, Indraja V, Krishna VH. A review on small scale wind turbines. Renew Sustain Energy Rev 2016;56:1351–71. http://dx.doi.org/10.1016/j.rser.2015.12.027.

[19] Jin X, Zhao G, Gao K, Ju W. Darrieus vertical axis wind turbine: basic research methods. Renew Sustain Energy Rev 2015;42:212–25. http://dx.doi.org/10.1016/j.rser.2014.10.021.

[20] Wong KH, Chong WT, Sukiman NL, Poh SC, Shiah Y-C, Wang C-T. Performance enhancements on vertical axis wind turbines using flow augmentation systems: a review. Renew Sustain Energy Rev 2017;73:904–21. http://dx.doi.org/10.1016/j.rser.2017.01.160.

[21] Liu WY. A review on wind turbine noise mechanism and de-noising techniques. Renew Energy 2017. http://dx.doi.org/10.1016/j.renene.2017.02.034.

[22] Sanderse B, van der Pijl SP, Koren B. Review of computational fluid dynamics for wind turbine wake aerodynamics. Wind Energy 2011;14:799–819. http://dx.doi.org/10.1002/we.

[23] Miller A, Chang B, Issa R, Chen G. Review of computer-aided numerical simulation in wind energy. Renew Sustain Energy Rev 2013;25:122–34. http://dx.doi.org/10.1016/j.rser.2013.03.059.

[24] Blazek J. Computational fluid dynamics: principles and applications. Elsevier Ltd; 2015.

[25] Danao LA, Edwards J, Eboibi O, Howell R. A numerical investigation into the influence of unsteady wind on the performance and aerodynamics of a vertical axis wind turbine. Appl Energy 2014;116:111–24. http://dx.doi.org/10.1016/j.apenergy.2013.11.045.

[26] Zadeh SN, Komeili M, Paraschivoiu M. Mesh convertence study for 2-D straight-blade vertical axis wind turbine simulations and estimation for 3-D simulations. Can Society Mech Eng 2014;38:487–504.

[27] Balduzzi F, Bianchini A, Ferrara G, Ferrari L. Dimensionless numbers for the assessment of mesh and timestep requirements in CFD simulations of Darrieus wind turbines. Energy 2016;97:246–61. http://dx.doi.org/10.1016/j.energy.2015.12.111.

[28] Song C, Zheng Y, Zhao Z, Zhang Y, Li C, Jiang H. Investigation of meshing strategies and turbulence models of computational fluid dynamics simulations of vertical axis wind turbines. J Renew Sustain Energy 2015;7. http://dx.doi.org/10.1063/1.4921578.

[29] Zadeh SN, Komeili M, Paraschivoiu M. Mesh convergence study for 2-D straight-blade vertical axis wind turbine simulations and estimation for 3-D simulations. Trans Can Soc Mech Eng 2014;38:487–504.

[30] Alaimo A, Esposito A, Messineo A, Orlando C, Tumino D. 3D CFD analysis of a vertical axis wind turbine. Energies 2015;8:3013–33. http://dx.doi.org/10.3390/en8043013.

[31] Nobile R, Vahdati M, Barlow JF, Mewburn-Crook A. Unsteady flow simulation of a vertical axis augmented wind turbine: a two-dimensional study. J Wind Eng Ind Aerodyn 2014;125:168–79. http://dx.doi.org/10.1016/j.jweia.2013.12.005.

[32] Lanzafame R, Mauro S, Messina M. 2D CFD modeling of H-Darrieus Wind Turbines using a transition turbulence model. Energy Procedia 2014;45:131–40. http://dx.doi.org/10.1016/j.egypro.2014.01.015.

[33] Raciti Castelli M, Englaro A, Benini E. The Darrieus wind turbine: proposal for a new performance prediction model based on CFD. Energy 2011;36:4919–34. http://dx.doi.org/10.1016/j.energy.2011.05.036.

[34] Chen J, Chen L, Xu H, Yang H, Ye C, Liu D. Performance improvement of a vertical axis wind turbine by comprehensive assessment of an airfoil family. Energy 2016;114:318–31. http://dx.doi.org/10.1016/j.energy.2016.08.005.

[35] Castelli MR, Ardizzon G, Battisti L, Benini E, Pavesi G. Modeling Strategy and Numerical Validation. Proc ASME 2010 Int Mech Eng Congr Expo 2010:1–10.

[36] Ferreira CJS, Bijl H, Van Bussel G, Van Kuik G. Simulating dynamic stall in a 2D VAWT: modeling strategy, verification and validation with particle image velocimetry data. J Phys: Conf Ser 2007;75:12023. http://dx.doi.org/10.1088/1742-6596/75/1/012023.

[37] Mohamed MH. Performance investigation of H-rotor Darrieus turbine with new airfoil shapes. Energy 2012;47:522–30. http://dx.doi.org/10.1016/j.energy.2012.08.044.

[38] Rezaeiha A, Kalkman I, Blocken B. CFD simulation of a vertical axis wind turbine operating at a moderate tip speed ratio: guidelines for minimum domain size and azimuthal increment. Renew Energy 2017;107:373–85. http://dx.doi.org/10.1016/j.renene.2017.02.006.

[39] Yakhot V, Orszag SA. Renormalization group analysis of turbulence. I. Basic theory. J Sci Comput 1986;1:3–51. http://dx.doi.org/10.1007/BF01061452.

[40] Orszag SA, Yakhot V, Flannery WS, Boysan F, Choudhury D, Maruzewski J, et al. Renormalization group modeling and turbulence simulations, Tempe, Arizona: 1993.

[41] Shih TH, Liou WW, Shabbir A, Yang Z, Zhu J. A new K-epsilon eddy viscosity model for high reynolds number turbulent flows: model development and validation. Comput Fluids 1995;24:227–38. http://dx.doi.org/10.1016/0045-7930(94)00032-T.

[42] Menter FR. Two-equation eddy-eiscosity turbulence models for engineering applications. AIAA J 1994;32:1598–605. http://dx.doi.org/10.2514/3.12149.

[43] Johnson DA, King LS. A mathematically simple turbulence closure model for attached and separated turbulent boundary layers. AIAA J 1985;23:1684–92. http://dx.doi.org/10.2514/3.9152.

[44] Bedon G, De Betta S, Benini E. A computational assessment of the aerodynamic performance of a tilted Darrieus wind turbine. J Wind Eng Ind Aerodyn 2015;145:263–9. http://dx.doi.org/10.1016/j.jweia.2015.07.005.

[45] Almohammadi KM, Ingham DB, Ma L, Pourkashanian M. Modeling dynamic stall of a straight blade vertical axis wind turbine. J Fluids Struct 2015;57:144–58. http://dx.doi.org/10.1016/j.jfluidstructs.2015.06.003.

[46] Bianchini A, Ferrara G, Ferrari L. Pitch optimization in small-size Darrieus wind turbines. Energy Procedia 2015;81:122–32. http://dx.doi.org/10.1016/j.egypro.2015.12.067.

[47] Lam HF, Peng HY. Study of wake characteristics of a vertical axis wind turbine by two- and three-dimensional computational fluid dynamics simulations. Renew Energy 2016;90:386–98. http://dx.doi.org/10.1016/j.renene.2016.01.011.

[48] Li C, Zhu S, Xu Y-L, Xiao Y. 2.5D large eddy simulation of vertical axis wind turbine in consideration of high angle of attack flow. Renew Energy 2013;51:317–30. http://dx.doi.org/10.1016/j.renene.2012.09.011.

[49] Elkhoury M, Kiwata T, Aoun E. Experimental and numerical investigation of a three-dimensional vertical-axis wind turbine with variable-pitch. J Wind Eng Ind Aerodyn 2015;139:111–23. http://dx.doi.org/10.1016/j.jweia.2015.01.004.

[50] Peng HY, Lam HF. Turbulence effects on the wake characteristics and aerodynamic performance of a straight-bladed vertical axis wind turbine by wind tunnel tests and large eddy simulations. Energy 2016;109:557–68. http://dx.doi.org/10.1016/j.energy.2016.04.100.

[51] Ghasemian M, Nejat A. Aero-acoustics prediction of a vertical axis wind turbine using Large Eddy Simulation and acoustic analogy. Energy 2015;88:711–7. http://dx.doi.org/10.1016/j.energy.2015.05.098.

[52] Verhoeven O. Trailing edge noise simulations. Thesis 2011:1–139.

[53] Lei H, Zhou D, Bao Y, Li Y, Han Z. Three-dimensional Improved Delayed Detached Eddy Simulation of a two-bladed vertical axis wind turbine. Energy Convers Manage 2017;133:235–48. http://dx.doi.org/10.1016/j.enconman.2016.11.067.

[54] Sabaeifard P, Razzaghi H, Forouzandeh A. Determination of vertical axis wind turbines optimal configuration through CFD simulations. 2012 Int Conf Futur Environ Energy 2012;2012(28):109–13.

[55] Lee YT, Lim HC. Numerical study of the aerodynamic performance of a 500 W Darrieus-type vertical-axis wind turbine. Renew Energy 2015;83:407–15. http://dx.doi.org/10.1016/j.renene.2015.04.043.

[56] Gang D, Kau WC. Unsteady flow numerical simulation of vertical axis wind turbine. Procedia Eng 2015;99:734–40. http://dx.doi.org/10.1016/j.proeng.2014.12.595.

[57] Gosselin R, Dumas G, Boudreau M. Parametric study of H-Darrieus vertical-axis turbines using CFD simulations. J Renew Sustain Energy 2016;8. http://dx.doi.org/10.1063/1.4963240.
[58] Castelli M, De Betta S, Bernini E. Effect of blade number on a straight-bladed vertical axis wind turbine. World Acad Sci Eng Technol 2012;61:305–11.
[59] Mohamed MH, Ali AM, Hafiz AA. CFD analysis for H-rotor Darrieus turbine as a low speed wind energy converter. Eng Sci Technol Int J 2015;18:1–13. http://dx.doi.org/10.1016/j.jestch.2014.08.002.
[60] Bausas MD, Danao LAM. The aerodynamics of a camber-bladed vertical axis wind turbine in unsteady wind. Energy 2015;93:1155–64. http://dx.doi.org/10.1016/j.energy.2015.09.120.
[61] Sengupta AR, Biswas A, Gupta R. Studies of some high solidity symmetrical and unsymmetrical blade H-Darrieus rotors with respect to starting characteristics, dynamic performances and flow physics in low wind streams. Renew Energy 2016;93:536–47. http://dx.doi.org/10.1016/j.renene.2016.03.029.
[62] Castelli MR, Benini E. Effect of blade inclination angle on a Darrieus wind turbine. J Turbomach 2012;134:31016. http://dx.doi.org/10.1115/1.4003212.
[63] Li Q, Maeda T, Kamada Y, Murata J, Kawabata T, Shimizu K, et al. Wind tunnel and numerical study of a straight-bladed Vertical Axis Wind Turbine in three-dimensional analysis (Part II: For predicting flow field and performance). Energy 2016;104:295–307. http://dx.doi.org/10.1016/j.energy.2016.03.129.
[64] Li Q, Maeda T, Kamada Y, Murata J, Kawabata T, Shimizu K, et al. Wind tunnel and numerical study of a straight-bladed vertical axis wind turbine in three-dimensional analysis (Part I: For predicting aerodynamic loads and performance). Energy 2016;106:443–52. http://dx.doi.org/10.1016/j.energy.2016.03.089.
[65] Bedon G, De Betta S, Benini E. Performance-optimized airfoil for Darrieus wind turbines. Renew Energy 2016;94:328–40. http://dx.doi.org/10.1016/j.renene.2016.03.071.
[66] Ismail MF, Vijayaraghavan K. The effects of aerofoil profile modification on a vertical axis wind turbine performance. Energy 2015;80:20–31. http://dx.doi.org/10.1016/j.energy.2014.11.034.
[67] Jafaryar M, Kamrani R, Gorji-Bandpy M, Hatami M, Ganji DD. Numerical optimization of the asymmetric blades mounted on a vertical axis cross-flow wind turbine. Int Commun Heat Mass Transf 2016;70:93–104. http://dx.doi.org/10.1016/j.icheatmasstransfer.2015.12.003.
[68] Zamani M, Maghrebi MJ, Varedi SR. Starting torque improvement using J-shaped straight-bladed Darrieus vertical axis wind turbine by means of numerical simulation. Renew Energy 2016;95:109–26. http://dx.doi.org/10.1016/j.renene.2016.03.069.
[69] Zamani M, Nazari S, Moshizi SA, Maghrebi MJ. Three dimensional simulation of J-shaped Darrieus vertical axis wind turbine. Energy 2016;116:1243–55. http://dx.doi.org/10.1016/j.energy.2016.10.031.
[70] Dabiri JO. Potential order-of-magnitude enhancement of wind farm power density via counter-rotating vertical-axis wind turbine arrays. J Renew Sustain Energy 2011;3. http://dx.doi.org/10.1063/1.3608170.
[71] Park J, Law KH. Layout optimization for maximizing wind farm power production using sequential convex programming. Appl Energy 2015;151:320–34. http://dx.doi.org/10.1016/j.apenergy.2015.03.139.
[72] Barthelmie RJ, Pryor SC. An overview of data for wake model evaluation in the Virtual Wakes Laboratory. Appl Energy 2013;104:834–44. http://dx.doi.org/10.1016/j.apenergy.2012.12.013.
[73] Xydis G, Koroneos C, Loizidou M. Exergy analysis in a wind speed prognostic model as a wind farm sitting selection tool: a case study in Southern Greece. Appl Energy 2009;86:2411–20. http://dx.doi.org/10.1016/j.apenergy.2009.03.017.
[74] Giorgetti S, Pellegrini G, Zanforlin S. CFD investigation on the aerodynamic interferences between medium-solidity Darrieus Vertical Axis Wind Turbines. Energy Procedia 2015;81:227–39. http://dx.doi.org/10.1016/j.egypro.2015.12.089.
[75] Chen W-H, Chen C-Y, Huang C-Y, Hwang C-J. Power output analysis and optimization of two straight-bladed vertical-axis wind turbines. Appl Energy 2017;185:223–32. http://dx.doi.org/10.1016/j.apenergy.2016.10.076.
[76] Zanforlin S, Nishino T. Fluid dynamic mechanisms of enhanced power generation by closely spaced vertical axis wind turbines. Renew Energy 2016;99:1213–26. http://dx.doi.org/10.1016/j.renene.2016.08.015.
[77] Chowdhury H, Mustary I, Loganathan B, Alam F. Adjacent wake effect of a vertical axis wind turbine. Procedia Eng 2015;105:692–7. http://dx.doi.org/10.1016/j.proeng.2015.05.058.
[78] Pinder N. Mechanical noise from wind turbines; 1993.
[79] Iida A, Mizuno A, Fukudome K. Numerical simulation of aerodynamic noise radiated form vertical axis wind turbines. Int Congr Acoust 2004:1–4.
[80] Mohamed MH. Aero-acoustics noise evaluation of H-rotor Darrieus wind turbines. Energy 2014;65:596–604. http://dx.doi.org/10.1016/j.energy.2013.11.031.
[81] Mohamed MH. Reduction of the generated aero-acoustics noise of a vertical axis wind turbine using CFD (Computational Fluid Dynamics) techniques. Energy 2016;96:531–44. http://dx.doi.org/10.1016/j.energy.2015.12.100.
[82] Scheurich F, Brown RE. Vertical-axis wind turbines in oblique flow: sensitivity to rotor geometry. Eur Wind Energy Conf Exhib 2011, EWEC 2011 2011:222–5.
[83] Tabrizi AB, Whale J, Lyons T, Urmee T. Performance and safety of rooftop wind turbines: use of CFD to gain insight into inflow conditions. Renew Energy 2014;67:242–51. http://dx.doi.org/10.1016/j.renene.2013.11.033.
[84] Bhargav MMSRS, Ratna Kishore V, Laxman V. Influence of fluctuating wind conditions on vertical axis wind turbine using a three dimensional CFD model. J Wind Eng Ind Aerodyn 2016;158:98–108. http://dx.doi.org/10.1016/j.jweia.2016.10.00.
[85] Wekesa DW, Wang C, Wei Y, Danao LAM. Analytical and numerical investigation of unsteady wind for enhanced energy capture in a fluctuating free-stream. Energy 2017;121:854–64. http://dx.doi.org/10.1016/j.energy.2017.01.041.
[86] Chowdhury AM, Akimoto H, Hara Y. Comparative CFD analysis of vertical axis wind turbine in upright and tilted configuration. Renew Energy 2016;85:327–37. http://dx.doi.org/10.1016/j.renene.2015.06.037.
[87] Orlandi A, Collu M, Zanforlin S, Shires A. 3D URANS analysis of a vertical axis wind turbine in skewed flows. J Wind Eng Ind Aerodyn 2015;147:77–84. http://dx.doi.org/10.1016/j.jweia.2015.09.010.
[88] Shahzad A, Asim T, Mishra R, Paris A. Performance of a vertical axis wind turbine under accelerating and decelerating flows. Procedia CIRP 2013;11:311–6. http://dx.doi.org/10.1016/j.procir.2013.07.006.
[89] Siddiqui MS, Rasheed A, Kvamsdal T, Tabib M. Effect of turbulence intensity on the performance of an offshore vertical axis wind turbine. Energy Procedia 2015;80:312–20. http://dx.doi.org/10.1016/j.egypro.2015.11.435.
[90] Lei H, Zhou D, Lu J, Chen C, Han Z, Bao Y. The impact of pitch motion of a platform on the aerodynamic performance of a floating vertical axis wind turbine. Energy 2017;119:369–83. http://dx.doi.org/10.1016/j.energy.2016.12.086.
[91] Chong WT, Fazlizan A, Poh SC, Pan KC, Hew WP, Hsiao FB. The design, simulation and testing of an urban vertical axis wind turbine with the omni-direction-guide-vane. Appl Energy 2013;112:601–9. http://dx.doi.org/10.1016/j.apenergy.2012.12.064.
[92] Lim YC, Chong WT, Hsiao FB. Performance investigation and optimization of a vertical axis wind turbine with the omni-direction-guide-vane. Procedia Eng 2013;67:59–69. http://dx.doi.org/10.1016/j.proeng.2013.12.005.
[93] Shahizare B, Nik-Ghazali N, Chong WT, Tabatabaeikia S, Izadyar N, Esmaeilzadeh A. Novel investigation of the different Omni-direction-guide-vane angles effects on the urban vertical axis wind turbine output power via three-dimensional numerical simulation. Energy Convers Manage 2016;117:206–17. http://dx.doi.org/10.1016/j.enconman.2016.03.034.
[94] Zanforlin S, Letizia S. Improving the performance of wind turbines in urban environment by integrating the action of a diffuser with the aerodynamics of the rooftops. Energy Procedia 2015;82:774–81. http://dx.doi.org/10.1016/j.egypro.2015.11.810.
[95] Rossetti A, Pavesi G. Comparison of different numerical approaches to the study of the H-Darrieus turbines start-up. Renew Energy 2013;50:7–19. http://dx.doi.org/10.1016/j.renene.2012.06.025.
[96] Asr MT, Nezhad EZ, Mustapha F, Wiriadidjaja S. Study on start-up characteristics of H-Darrieus vertical axis wind turbines comprising NACA 4-digit series blade airfoils. Energy 2016;112:528–37. http://dx.doi.org/10.1016/j.energy.2016.06.059.